Accepted Manuscript

A theoretical and computational study of the high-temperature effects on the transition criteria of shock wave reflections

Peng Jun, Zhang Zijian, Hu Zongmin, Jiang Zonglin

PII: S1270-9638(18)32299-5
DOI: https://doi.org/10.1016/j.ast.2019.03.021
Reference: AESCTE 5052

To appear in: *Aerospace Science and Technology*

Received date: 18 October 2018
Revised date: 22 January 2019
Accepted date: 6 March 2019

Please cite this article in press as: P. Jun et al., A theoretical and computational study of the high-temperature effects on the transition criteria of shock wave reflections, *Aerosp. Sci. Technol.* (2019), https://doi.org/10.1016/j.ast.2019.03.021

A theoretical and computational study of the high-temperature effects on the transition criteria of shock wave reflections

Peng Jun [a,b], Zhang Zijian [a,b], Hu Zongmin [a,b*], Jiang Zonglin [a,b]

[a] State Key Laboratory of High temperature Gas Dynamics, Institute of Mechanics, Chinese Academy of Sciences, Beijing 100190, China;

[b] School of Engineering Science, University of Chinese Academy of Sciences, Beijing 100049, China

Abstract: In this paper, we study the high-temperature effects on the reflection of shock waves in hypersonic flows by using analytical and computational approaches. First, a theoretical approach is established to solve the shock relations which are further applied to develop the shock polar analytical method for high-temperature air. Then, a comparative investigation using ideal gas model and real gas model considering vibration excitation indicates that the high-temperature effects cause an obvious change to the overall profile of the shock polar. The post-shock pressure increases within the strong branch of the shock polar while decreases within the weak branch due to vibration excitation of air molecules. A more notable phenomenon is the increase in the maximum deflection angle of the shock polar which can significantly influence the detachment criterion of shock reflection transition in high-temperature air flows. The shock polar analysis of shock reflection

shows that the high-temperature effects result in an obvious increase to the detachment criterion while a slight increase to the von Neumann criterion. A series of computations are conducted to confirm the above analytical findings on the shock reflection considering high-temperature effects. A slight difference of transition criterion between the theory and computations is found to be caused by the existence of the expansion fan which is an inherent flow structure. The proposed shock polar analytical method is proved to be an effective but simple approach for the study of shock wave reflections in hypersonic flows.

Keywords: shock reflection; vibration excitation; Mach reflection; transition criterion; hypersonic flow

1 Introduction

The reflection of shock waves is an important phenomenon in steady supersonic flows[1]. The study of shock reflection can be traced back to more than one hundred years when Mach observed two different reflection configurations: regular reflection (RR) and Mach reflection (MR)[2]. After 70 years, von Neumann discovered the secret of the shock reflection and proposed the two-and-three-shock theory which became a powerful tool for analyzing shock reflection. At the same time, he provided two criteria known as the mechanical equilibrium criterion (or von Neumann criterion) and the detachment criterion. The former defines the minimum angle of incidence θ_N for the theoretical existence of MR, while the latter gives the maximal angle θ_D for RR. Moreover, when the flow Mach number Ma is larger than 2.2 for the calorically perfect gas with the specific heat ratio γ=1.4, there is a range of angles of incidence $\theta_N < \theta_D$ (dual solution domain) where both RR and MR are theoretically possible. Because of

the magical existence of a dual solution domain, many scientists were attracted to research the transition between RR and MR. Horning proposed that the existence of the dual solution domain implied there might be a hysteresis phenomenon at the transition[3]. He assumed the transition from RR to MR would happen until the incidence angle increased to θ_D. The Mach stem would arise suddenly and grow up at this angle. When the angle decreased, the MR should persist throughout the dual solution domain and become RR at the angle θ_N. However, the confirmation of this hypothesis did not go well until Chpoun[4] observed it in experiments and Ivanov[5] in numerical simulations of the same ages. After that, more and more investigations about the shock reflection[6-8] and the transition between RR and MR emerged to enrich such an issue.

The shock reflection problem has been extensively studied not only for its important flow physics but also for its strong engineering application background. For example, at the wing and inlet of a hypersonic vehicle, the reflection of shock wave may interact with the boundary layer on the wall[9-12], which may cause the problems of flow separation, unsteady motion, vortex motion, mixing, and turbulence, etc. On the contrary, in the scramjet inlet and Isolation section, we need shock wave reflected continuously on the upper and lower wall to complete the flow compression process[13, 14]. Another instance is that the shock wave reflection in premixed combustible gases can form high-temperature and high-pressure zone locally, which can make detonation ignition directly or through deflagration-to-detonation transition[15-17]. In a word, the application of shock reflection in engineering relies on a clear understanding of the characteristics of shock wave reflection configurations and their mechanisms, as well as the transition conditions between regular reflection and Mach reflection.

With the development of flight technologies, the Mach number of the vehicle has

entered the hypersonic field. After a hypersonic flow compressed by a single shock or even multiple shock waves, its huge kinetic energy may convert into internal energies leading to a sharp rise in temperature. A gas like air at such a high temperature will appear the molecular vibration excitation, dissociation, ionization and thermal chemical reaction, showing the different characteristics from the gas, which is called high-temperature or real gas effects[18, 19]. Therefore, the relationship between the shock wave and thermodynamic parameters will change when we take account of the high-temperature effects, which will influence the transition criteria of shock reflection. However, the transition criteria are important references for the design of a hypersonic vehicle as the flow field of RR is extra different from that of MR. Hence, it is of great significance to study detailed mechanism of high-temperature gas effects on the transition of shock reflection in order to complete the shock reflection theory at high Mach numbers and solve complicated engineering application problems.

Table 1 Thermochemical reaction process in each temperature range.

Temperature range /K	Thermochemical reaction process
<800	Calorically perfect gas
800~2500	Vibration excitation
2500~4000	O_2 begins to dissociate
4000~9000	N_2 begins to dissociate; O_2 almost completely dissociated
>9000	N_2 almost completely dissociated; Ionization begins

The underlying physical phenomena of high-temperature effects encompass vibrational excitation, dissociation, ionization, which occur sequentially as the gas temperature rises. The temperature ranges for the above phenomena are the list in Table 1 for air. It can be seen that vibrational excitation sustains in the range of 800-

2,500 K while dissociation of oxygen molecule takes place within 2,500-4,000 K.

Schematic illustrations of the wave configurations of regular reflection and Mach reflection are shown in figure 1. The labels, ①,②,③,④, respectively represent four flow states including the freestream flow as well as the flows downstream the incident shock (IS), the reflected shock (RS) and the Mach stem (MS). Ma_1, Ma_2, Ma_3, and Ma_4 denote the Mach numbers of the aforementioned flow states, respectively. θ_1 and θ_2 are the flow deflection angles across IS and RS while β_1 and β_2 are the incident shock angle and reflected shock angle

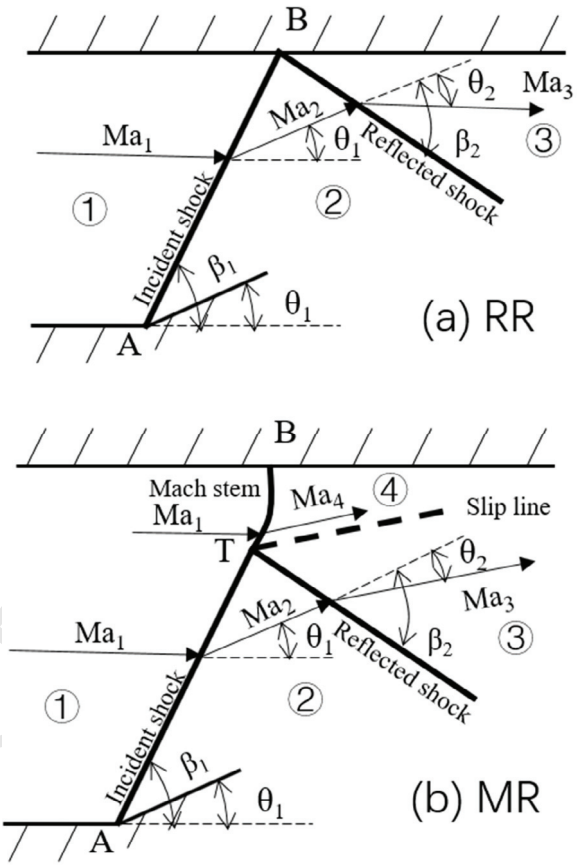

Figure 1 Schematic illustrations of shock reflection.

2 Thermodynamic model

The internal energy e and enthalpy h per unit mass containing the vibration energy, which appears different from that of a calorically perfect gas, are as follow,

$$\mathrm{e}(T)=\frac{3}{2}RT+RT+R\frac{T_{\mathrm{ve}}}{e^{T_{\mathrm{ve}}/T}-1}, \tag{1}$$

$$h(T)=e(T)+RT, \tag{2}$$

where R is the gas constant, and T_{ve} is the characteristic temperature of vibration. The three terms on the right-hand side of eq. (1) are the energies of molecular translational, rotational and vibration, respectively. From the above equations, we can get the specific heat at constant volume and constant pressure, c_V, and c_P,

$$c_V=\frac{3}{2}R+R+R\left(\frac{T_{\mathrm{ve}}}{T}\right)^2\frac{e^{T_{\mathrm{ve}}/T}}{\left(e^{T_{\mathrm{ve}}/T}-1\right)^2}, \tag{3}$$

$$c_P=c_V+R. \tag{4}$$

For air approximately consisting 79% N_2 and 21% O_2, the relative thermodynamic quantities will be

$$\begin{aligned}e(T)=&\frac{5}{2}R_{\mathrm{air}}T+m_{\mathrm{N_2}}\cdot R_{\mathrm{N_2}}\frac{T_{\mathrm{ve,N_2}}}{e^{T_{\mathrm{ve,N_2}}/T}-1}\\&+m_{\mathrm{O_2}}\cdot R_{\mathrm{O_2}}\frac{T_{\mathrm{ve,O_2}}}{e^{T_{\mathrm{ve,O_2}}/T}-1},\end{aligned} \tag{5}$$

$$\begin{aligned}c_V=&\frac{5}{2}R_{\mathrm{air}}+m_{\mathrm{N_2}}\cdot R_{\mathrm{N_2}}\left(\frac{T_{\mathrm{ve,N_2}}}{T}\right)^2\frac{e^{T_{\mathrm{ve,N_2}}/T}}{\left(e^{T_{\mathrm{ve,N_2}}/T}-1\right)^2}\\&+m_{\mathrm{O_2}}\cdot R_{\mathrm{O_2}}\left(\frac{T_{\mathrm{ve,O_2}}}{T}\right)^2\frac{e^{T_{\mathrm{ve,O_2}}/T}}{\left(e^{T_{\mathrm{ve,O_2}}/T}-1\right)^2},\end{aligned} \tag{6}$$

$$c_P=c_V+R_{air}, \tag{7}$$

$$\gamma=\frac{c_P(T)}{c_V(T)}=\gamma(T), \qquad (8)$$

where R_{air}, R_{N2}, and R_{O2} are the gas constant of air, N_2, and O_2 while mN_2 and mO_2 are mass fractions of N_2 and O_2. As each of the following thermodynamic parameters, c_V, c_P and specific heat ratio γ, is a single argument function of temperature T, the general state equation is still suitable

$$p=\rho RT. \qquad (9)$$

The relation of enthalpy h and special heat ratio γ with the temperature of the air can be illustrated in figure 2. In Figure 2, the dashed and solid lines represent the enthalpy of calorically perfect gas and real gas, and dash-dot lines represent the specific heat ratio, respectively. It can be seen from this figure that, above 600K, the effect of vibration excitation on the enthalpy is obvious, and it becomes larger as the temperature rises. The ratio of vibration energy to enthalpy increases to 10.7% at 2000 K. What's more, the specific heat ratio changes from 1.4 to about 1.3 as the temperature rises. The change of γ across a shock wave in a real gas will directly lead to changes of pressure, density and temperature ratios as compared with cases for constant γ.

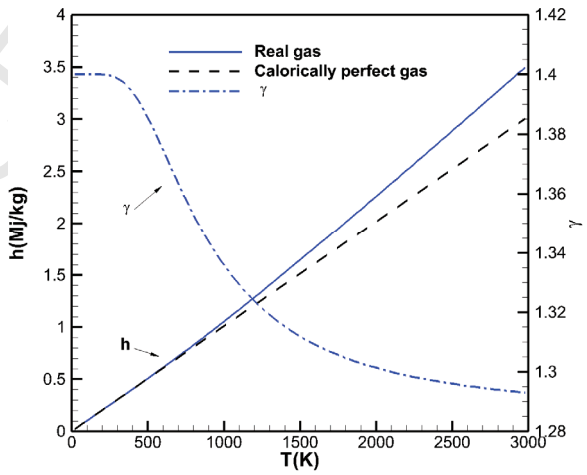

Figure 2 Enthalpy and specific heat ratio for the high-temperature air

3. The theoretical solution to shock wave reflection

3.1 Shock relation

The influence of the high-temperature gas effect on the thermodynamic properties will change the relation of the physical variables before and after the shock. The control equations for a normal shock wave in a real gas are as follows,

$$\rho_1 u_1 = \rho_2 u_2, \qquad (10)$$

$$P_1 + \rho_1 u_1^2 = P_2 + \rho_2 u_2^2, \qquad (11)$$

$$h(T_1) + \frac{1}{2} u_1^2 = h(T_2) + \frac{1}{2} u_2^2, \qquad (12)$$

where P, ρ and u are pressure, density, and velocity. The subscript 1 and 2 respectively represent the flow states upstream and downstream of the shock wave. In the eq. (12), $h(T)$=e(T)+Rair•T. From the control equations, we can approximately analyze the influence of vibration excitation on the physical variables after the wave. Since the vibration energy is active, $h(T_2)$ for a real gas will increase as compared with that for an calorically perfect gas. This leads to the decline of velocity u_2 as shown in eq. (12). As the terms on the left-hand sides of eq. (10) and (11) are given, ρ_2 and P_2 will consequently increase for a normal shock wave.

We can get an exact solution by solving the control equations numerically. Assuming that the flow variables before the shock wave are known, solving the control equations we can get an equation about the velocity u_2 and the temperature T_2 downstream of the shock

$$f(u_2, T_2) = h(T_2) + \frac{1}{2} u_2^2 - h_1(T_1) - \frac{1}{2} u_1^2 = 0, \qquad (13)$$

where T_2 is

$$T_2 = \frac{1}{R}\left(\frac{RT_1}{u_1} + u_1 - u_2\right)u_2. \tag{14}$$

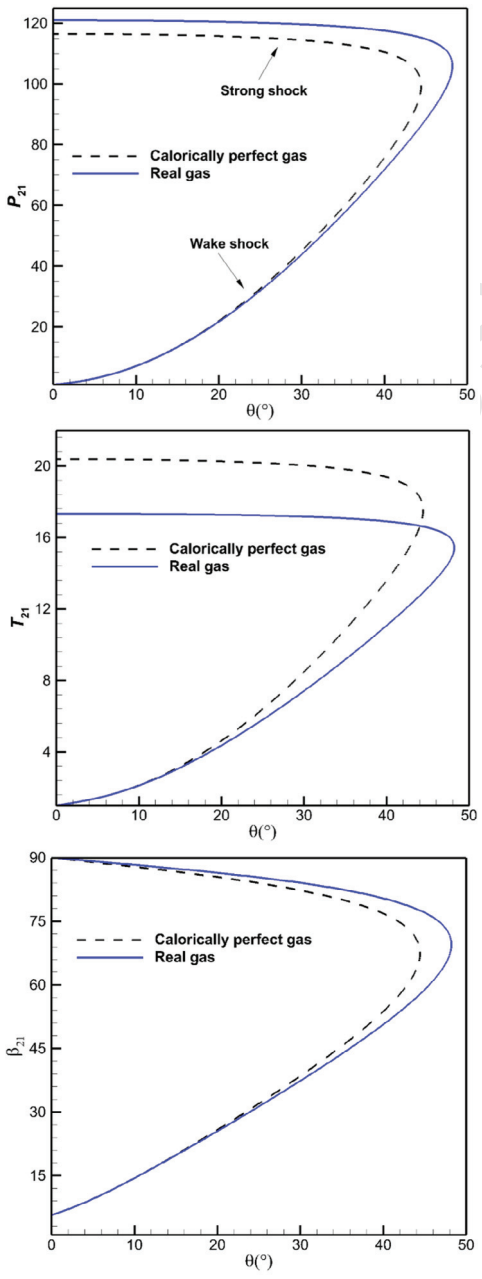

Figure 3 Shock polar for *Ma*=10.

We can use the Newton iterative method to obtain a numerical solution of u_2 and then

obtain other variables by the control equations. Considering the shock angle, the aforementioned iterative method can be extended to solve an oblique shock wave. Through the two-shock and three-shock theory of shock reflection proposed by von Neumann, we can find the key -relation among shock parameters is the flow deflection angle, θ, across a shock wave and the static pressure P downstream of the shock. So, the relation curve of θ_1 and P is proposed to analyze the oblique shock wave by Kawamura, and so on[20]. This curve was called shock polar later. After that, the shock polar became a powerful way to express the shock relation comprehensively.

As hypersonic vehicles always fly in the upper atmosphere, we take the air at 30 km above the sea level as the freestream flow condition where T=226K. We will use the same condition for the following cases hereinafter unless other statements. The shock polar considering the high-temperature effect are used to compare with that of the calorically perfect gas as depicted in Figure 3 for a Mach 10 hypersonic flow.

In Fig.3, P_{21}, T_{21} are respectively the ratios of pressure and temperature across the shock wave while β is the shock angle. Through Fig.3 (a), we can find the real gas effect makes the pressure decrease in the weak branch and increase in the strong branch. This is a very surprising phenomenon. The overall polar contour and the maximum flow deflection angle get larger when high-temperature effects are considered. As shown in Fig.3 (b), high-temperature effects cause a reduction in temperature in each branch as compared with the polar for the calorically perfect gas. In the figure, $T_{21} \approx 20$, which means $T_2 \approx 2400$ K. Such a temperature is not high enough to make O_2 dissociate. That is to say, vibration excitation, instead of dissociation, is the main effect of high-temperature gas in the studied cases.

3.2 Shock reflection

The increase of the maximum deflection angle, as illustrated in Fig.3, may affect the detachment criterion for shock wave reflection. It can be illustrated by the shock polar solution to the shock reflection in Fig.4. The freestream flow conditions are T_1=226 K and Ma_1=10, while the deflection angle θ_1 = 15°, 30°, and 40°, respectively.

The number 1,2,3,4 in Fig.4 respectively represent the flow states ①,②,③,④ as defined in Fig.1. Those graphs respectively indicate three situations: regular reflections (RR), in the dual solution domain and Mach reflection (MR). It can be seen that the most notable difference of the shock polar between the real gas and the calorically perfect gas is the maximum flow deflection angle, θ_{max}, across the reflected shock where θ_{max} for the former is obviously larger than that for the latter. Therefore, the critical flow deflection angle across the incident shock, θ_1, becomes larger when the polar of the reflected shock detaches from the Y-axis. According to the previous numerical solution of shock wave relation, we can get the angle of detachment criterion and mechanical equilibrium criterion as depicted in Fig. 5.

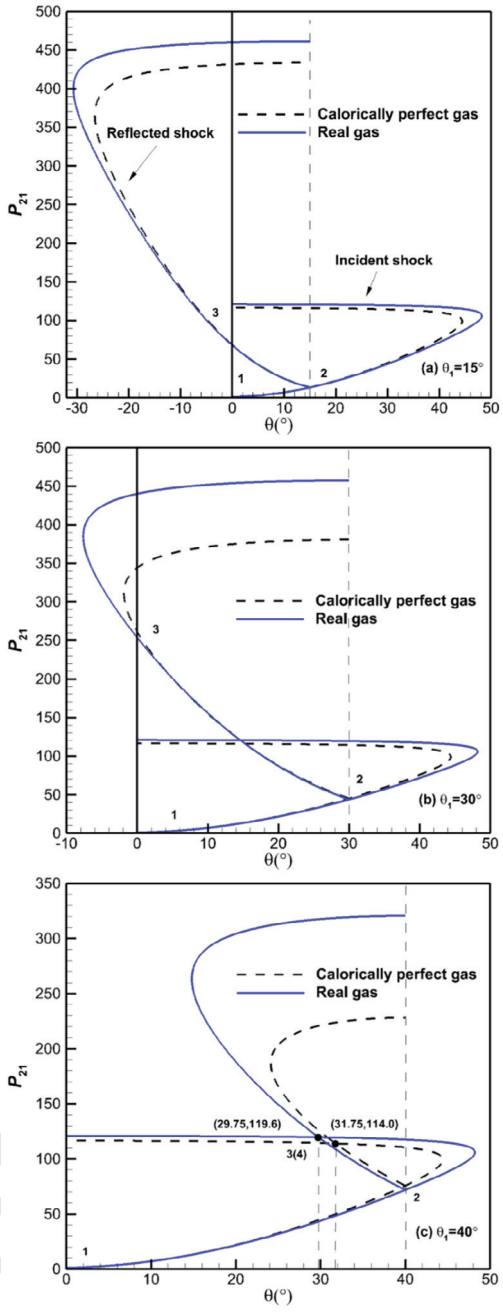

Figure 4 Polar solution to shock reflections.

These two figures show the transition criteria for the shock reflection in the freestream flows with T_1=60 K and 226 K, respectively. The lower curves in each frame indicate the angles of the von Neumann criterion, θ_N, and the curves of the upper part represent the angles of the detachment criterion, θ_D, in each frame. It can be seen from

the figures that there is a slight difference in θ_N criterion lines for two gas models. However, the difference in θ_D lines is obviously significant which is associated with the freestream flow temperature. The real gas effects postpone the transition from regular reflection to Mach reflection. What's more, the higher temperature of the freestream flows is, the more transition postpones.

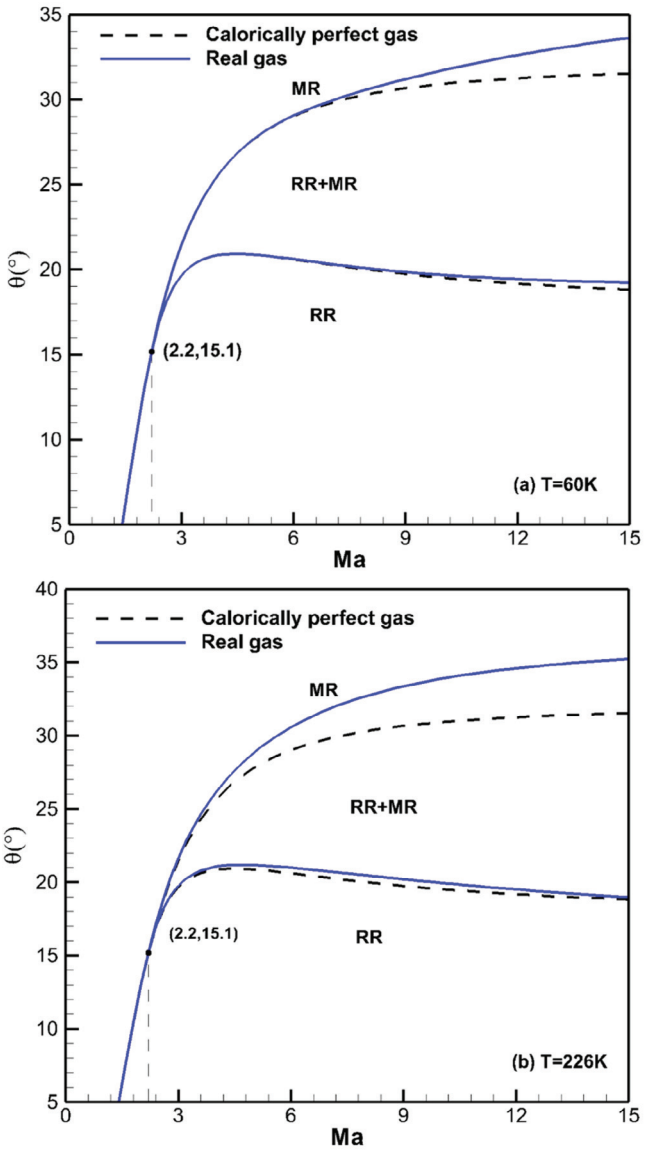

Figure 5 Transition criteria

4. Computational confirmation

4.1 Numerical method

The governing equation for shock reflection is the following 2D Euler equation,

$$\frac{\partial \boldsymbol{U}}{\partial t}+\frac{\partial \boldsymbol{F}}{\partial x}+\frac{\partial \boldsymbol{G}}{\partial y}=0, \qquad (15)$$

where U, F, and G are the unknown variables and fluxes in the x-, y- directions which are as follows,

$$\boldsymbol{U}=\begin{bmatrix}\rho C_1\\ \rho C_2\\ \rho u\\ \rho v\\ E\end{bmatrix},\boldsymbol{F}=\begin{bmatrix}\rho C_1 u\\ \rho C_2 u\\ \rho u^2+P\\ \rho uv\\ (E+P)u\end{bmatrix},\boldsymbol{G}=\begin{bmatrix}\rho C_1 v\\ \rho C_2 v\\ \rho vu\\ \rho v^2+P\\ (E+P)v\end{bmatrix}, \qquad (16)$$

where C_1 and C_2 are the mass fraction of O_2 and N_2. The total energy per unit mass E is

$$E=e(T)+\frac{1}{2}\left(u^2+v^2\right), \quad (17)$$

where internal energy $e(T)$ is given in eq. (5). For the real gas, the special heat ratio γ varies with temperature T.

The second-order DCD scheme is applied for the convective terms F and G. This scheme can effectively eliminate nonphysical oscillations near the discontinuities. For more details, refer to the literature[21].

4.2 Comparison of shock parameters

For conventional shock tunnels, the temperature and Mach number of freestream flows are generally too low to excite the vibration energy. However, for the aerodynamic properties of hypersonic vehicles, spacecraft and hypersonic shock tunnel,

the effect of high-temperature gas should be considered. The equilibrium vibration model without molecule dissociation and the calorically perfect gas model are applied in the following comparative computations to evaluate the gas model effects on the post-shock parameters. The freestream flow conditions for all the computations are given as a Mach 10 flight at 30 km in the atmosphere where T=226K. The flow deflection angle of the incident shock is θ=30° which is close to the corresponding detachment criterion. Along with numerical simulations, the theoretical calculation based on both gas models as mentioned above is conducted accordingly and given in Table 2 for comparison.

Table 2 Gas model effects on the reflected shock parameters

method	model	P_{21}	T_{21}	Ma_2	β_1	P_{31}	T_{31}	Ma_3	β_2
Theoretical	Calorically perfect gas	45.08	8.48	2.71	38.51	261.33	16.21	1.21	56.34
	Real gas	43.88	7.41	3.04	37.36	253.70	12.71	1.63	48.50
Simulation	Calorically perfect gas	45.18	8.49	2.71	38.99	264.21	16.19	1.22	56.56
	Real gas	43.83	7.40	3.05	37.40	253.18	12.58	1.65	48.27

The flow structure and the corresponding shock polar can be found in Fig.1 and Fig.4. respectively. Here, P_{21}, T_{21}, Ma_2, β_1 are flow parameters downstream of the incident shock wave, and P_{31}, T_{31}, Ma_3, β_2 are flow parameters downstream of the reflected shock wave. From the table, we can find that the results by both theoretical calculation and numerical simulation are almost same if using the same gas model while the differences between the data respectively achieved from the two gas models are significant. That is to say, the theoretical analysis method is accurate to capture the high-temperature effects on shock dynamics no matter which gas models is used.

Obviously, such a theoretical calculation is much more time-saving than computations. Additional simulations considering molecular dissociation besides vibrational excitation produce, however, almost the same data as the list in Table 2. The highest temperature after the reflected shock is about 2800 K, just a little larger than the beginning temperature of dissociation. That is to say, vibration excitation is the main effect of high-temperature gas and dissociating reaction can be ignored in the cases of interest in the present study. Therefore, we can close the dissociating reactions in all numerical simulations to better compare the theoretical and computational results.

4.3 Numerical simulation of shock reflection

We can use a simple way to find the critical angles of transition of shock reflection as follows: start at an angle of regular reflection until convergence, increase the deflection angle by 0.2°, then continue the calculation until convergence again, repeat the above conduction until a Mach reflection configuration appearing finally. In this way, we can get the detachment angle and then decrease the angle we can also get the von Neumann angle.

We use the same freestream flow conditions of the Mach 10 flight as mentioned above for the following simulations with calorically perfect gas and real gas model applied respectively.

First, for the grid independence study, a series of computations with the real gas model using different levels of grid density are conducted to compare the detached angles. The main features of the grid and the detached angles are summarized in Table 3. The detached angles based on the grid level 2 and 3 are the same which means that the grid independence is achieved. So, we chose the grid level 3 for the coming simulations.

Table 3 The grid main features

Grid level	Number of cells	Detached angle
1	300 x 200	35.1
2	600 x 380	34.7
3	1000 x 640	34.7

For simplicity, we only give the numerical illustration of the transition process for the case of the real gas model with Ma=10 as depicted in Fig. 6.

From the contour lines of the density, we can easily get the wave configuration of shock reflection. A Mach reflection configuration first occurs when the deflection angle is increased to θ=34.8°from 34.6°, so we take the average as the detachment angle, i.e., θ_D=34.7° where the error range of the detachment angle is 0.1°. In a similar way, we can get the von Neumann angle θv=19.5°. The numerical transition angles do not agree exactly with the theoretical angles (the theoretical angles is θv=19.9° and θ_D=33.9°). The numerical detachment angle is 0.8° higher than the theoretical one, and the numerical von Neumann angle is 0.4° lower than the theoretical one. Similar differences between the simulation and calculation also exist in the case of the calorically perfect gas model. The simulated result of the calorically perfect gas is θ_D=31.5° and θv=19.5°, however, the theoretical result is θ_D=30.9° and θv=19.5°. The difference between simulation and theory for the detachment angle is also reported in the literature[22]. We can get the computations of Ma=6, 8, 12 in the same way and combine the results in Fig. 7.

In Fig. 7, the squares and triangles indicate the simulated results using the real gas model and the calorically perfect gas model, respectively, while the solid and dashed lines represent the theoretical solutions using both gas models. From the illustration,

we can find the relations between the transition angle and Mach number are coincident with each other for the two methods applied in the present work. The computations confirm that the real gas model results in an obviously delayed transition from regular reflection to Mach reflection, i.e., the detachment criterion.

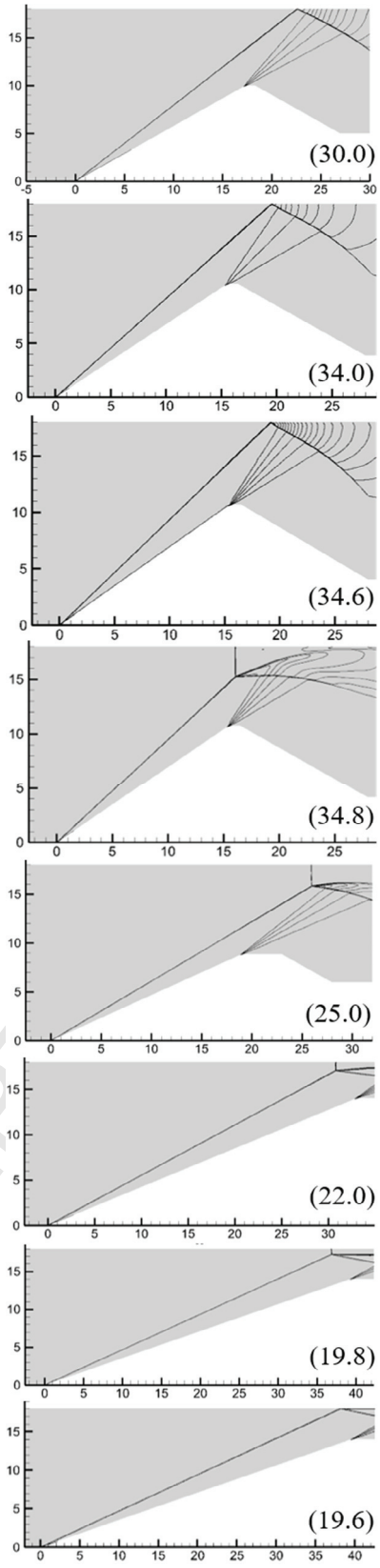

Figure 6 the transition of shock reflection (*Ma*=10).

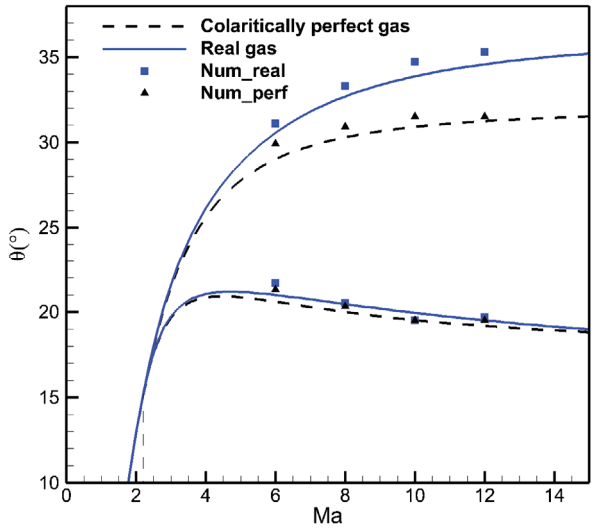

Figure 7 The transition angle of theory and simulation

There is a trouble in the above numerical simulations, the length of the wedge which leads to the flow deflection and also generates a series of expansion fans. The expansion fan originating from the wedge corner may weaken the incident shock wave and then influence the transition if the wedge is too short. In order to make the infecting field of expansion fans locate downstream of the reflection point to avoid the influence, we need a sufficient long wedge. On the contrary, we need the wedge as short as possible to get enough room for the forthcoming Mach reflection. Farther more, the oblique shock ware is very close to the wedge at a high Mach number. As a result, we cannot use a fixed length of the wedge for all the simulations and need to change the length slightly case by case.

4.4 The influence of expansion fans

From the Fig. 7, we find the squares and triangles are always above the lines about 0.6 degrees. These little but not negligible differences between the simulated results and theoretical solutions indicate that there might be some systematic errors in the

simulation. After analyzing the flow field, we guess it may be caused by the fans of expansion. Such a wave structure cannot be considered in the theoretical calculation and cannot be eliminated in a computation which may induce the difference mentioned above. Although the intersection of the reflected shock wave and the head of fans is behind the shock reflected point, the velocity of the flow behind the reflected shock wave is a little smaller than local velocity of sound. That is to say, the disturbance caused by the fans of expansion cross the reflected shock wave would spread upward to the reflected points. An effect of the expansion fans is making the flow deflecting coincidentally. It might increase the deflecting angle of flow after reflected shock wave which may make the existing of RR at the angle beyond the theoretical detached criterion.

In order to verify the guess, we need to conduct a supplementary simulation: just change the computational domain and leave other conditions unchanged. We cut off the most part of the computational domain behind the wedge to prevent the interaction between the expansion fan and the reflected shock wave along the right boundary. The wave structures for the case of Ma=10 are displayed in Fig.8 and indicate that the reflected shock wave and the expansion fan leave the right boundary without meeting each other. The RR to MR transition occurs when θ=34.1° based on the current simulations. A series of expansion fan-free simulations for different Mach numbers are conducted and the new obtained transition angles are depicted in Fig.9. As shown by the circle labels, the computational solutions become much closer to the theoretical criteria. The better agreement confirms our guess due to the fact that the influence of the expansion fan is not included in both theoretical solutions and the current computations. However, it should be pointed out that the expansion fans are always inherent flow structures in any real problems or experiments involving shock

reflections. Therefore, the slight difference of transition criterion between the theory and computations should not be surprising.

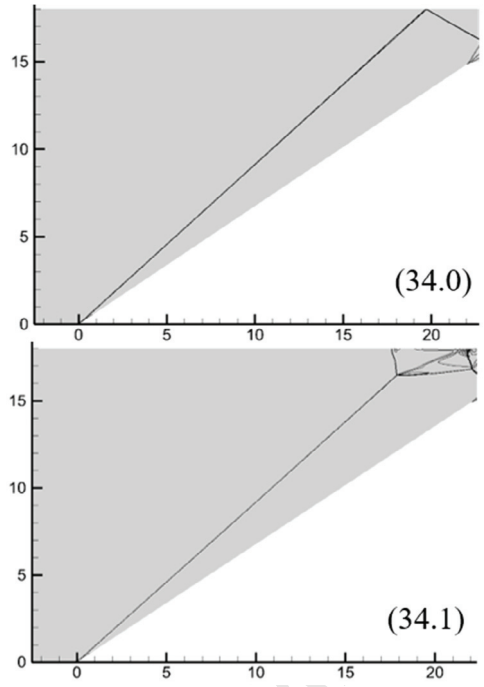

Figure 8 The RR to MR transition without expansion fans

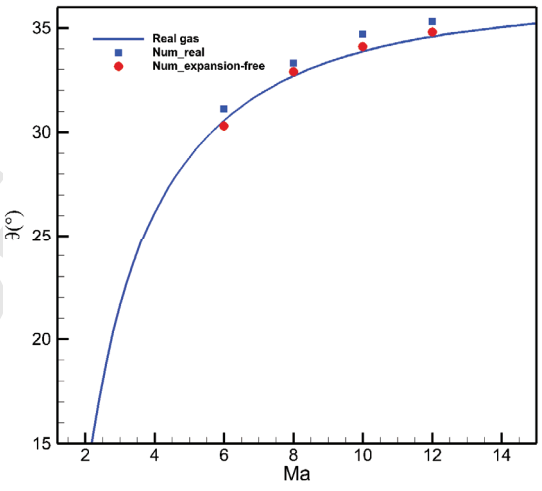

Figure 9 The corrected detached angle with Mach number

5 Conclusions

In the present paper, we have reviewed the research history of shock reflection and pointed out the critical problem of the shock reflection in hypersonic flow: the effect of high-temperature gas on the shock wave and its reflection. We developed a theoretical approach to rapidly solve the shock relation in real gases at the situation of vibration excitation. The obtained shock polar indicates that the effects of real gas result in opposite pressure changes to the strong branch and weak branch, i.e., an increase to the former and a decrease to the latter. In addition, the maximal deflection angle obtained by the polar using the real gas model becomes larger than the corresponding data for the calorically perfect gas model which should influence the detachment criterion of shock reflection transition.

A further investigation about the effect of vibration excitation on the transition of shock reflection indicates that vibration excitation makes the detached angle increase significantly while influences the von Neumann angle slightly. As for air, the vibration excitation makes the detached angle increase about 3.0° at Ma=10, and the increment increases with the increase of Mach number. Numerical simulations using both calorically perfect gas model and real gas mode confirm the above conclusions.

In the numerical simulation, we find the expansion fans originating from the wedge corner may postpone the transition from RR to MR. The expansion fans propagate across the reflected shock wave and make the flow deflect again to the mechanical balance when the deflection angle is a little larger than the detached angle. However, as the expansion fans are inescapable in experiments and reality applications, the slight difference of transition criterion between theory and computations is acceptable and coincident with the real flow physics.

Conflict of interest statement

There is no conflict of interest.

Acknowledgements

This work was supported by the National Natural Science Foundation of China under Grant No. 11672308 and 11532014.

References

[1] G. Ben-Dor, CHAPTER 8.1 - Oblique Shock Wave Reflections, in: G. Ben-Dor, O. Igra, T.O.V. Elperin (Eds.) Handbook of Shock Waves, Academic Press, Burlington, 2001, pp. 67-179.

[2] H. Hornung, Regular and Mach reflection of shock waves, Annual Review of Fluid Mechanics, 18 (1986) 33-58.

[3] H.G. Hornung, H. Oertel, R.J. Sandeman, Transition to Mach reflection of shock waves in steady and pseudo-steady flow with and without relaxation, Journal of Fluid Mechanics, 90 (1979) 541-560.

[4] B. Li, A. Chpoun, G. Ben-Dor, Analytical and experimental investigations of the reflection of asymmetric shock waves in steady flows, Journal of Fluid Mechanics, 390 (1999) 25-43.

[5] M.S. Ivanov, D. Vandromme, V.M. Fomin, A.N. Kudryavtsev, A. Hadjadj, D.V. Khotyanovsky, Transition between regular and Mach reflection of shock waves: new

numerical and experimental results, Shock Waves, 11 (2001) 199-207.

[6] F. Zhang, T. Si, Z. Zhai, X. Luo, J. Yang, X. Lu, Reflection of cylindrical converging shock wave over a plane wedge, Physics of Fluids, 28 (2016).

[7] H. Wang, Z. Zhai, X. Luo, J. Yang, X. Lu, A specially curved wedge for eliminating wedge angle effect in unsteady shock reflection, Physics of Fluids, 29 (2017).

[8] X. Shi, Y. Zhu, X. Luo, J. Yang, High temperature effects in moving shock reflection with protruding Mach stem, Theoretical and Applied Mechanics Letters, 6 (2016) 222-225.

[9] F.K. Lu, New results on the incipient separation of shock/boundary-layer interactions, in: J. Li, J. Fan (Eds.) Frontiers in Fluid Mechanics Research2015, pp. 12-15.

[10] V. Hermes, I. Klioutchnikov, H. Olivier, Numerical investigation of unsteady wave phenomena for transonic airfoil flow, Aerospace Science and Technology, 25 (2013) 224-233.

[11] M. Gageik, J. Nies, I. Klioutchnikov, H. Olivier, Pressure wave damping in transonic airfoil flow by means of micro vortex generators, Aerospace Science and Technology, 81 (2018) 65-77.

[12] C. Wang, C. Cheng, K. Cheng, L. Xue, Unsteady behavior of oblique shock train and boundary layer interactions, Aerospace Science and Technology, 79 (2018) 212-222.

[13] F. Falempin, R. Thevenot, a.P.P. Vancamberg, Hypersonic airbreathing propulsion - Flight test needs, International Aerospace Planes and Hypersonics Technologies,

American Institute of Aeronautics and Astronautics1995.

[14] L. Yue, Y. Jia, X. Xu, X. Zhang, P. Zhang, Effect of cowl shock on restart characteristics of simple ramp type hypersonic inlets with thin boundary layers, Aerospace Science and Technology, 74 (2018) 72-80.

[15] Y.P. Goonko, A.F. Latypov, I.I. Mazhul, A.M. Kharitonov, M.I. Yaroslavtsev, P. Rostand, Structure of Flow over a Hypersonic Inlet with Side Compression Wedges, AIAA Journal, 41 (2003) 436-447.

[16] Z. Jiang, K. Takayama, Reflection and focusing of toroidal shock waves from coaxial annular shock tubes, Computers & Fluids, 27 (1998) 553-562.

[17] F.K. Lu, H. Fan, D.R. Wilson, Detonation waves induced by a confined wedge, Aerospace Science and Technology, 10 (2006) 679-685.

[18] K. Izumi, S. Aso, M. Nishida, Experimental and computational studies focusing processes of shock waves reflected from parabolic reflectors, Shock Waves, 3 (1994) 213-222.

[19] H. Olivier, H. Groenig, Hypersonic model testing in a shock tunnel, 5th International Aerospace Planes and Hypersonics Technologies Conference, American Institute of Aeronautics and Astronautics1993.

[20] R. Kawamura, H. Saito, Reflection of shock waves-1 Pseudo-stationary case, Journal of the Physical Society of Japan, 11 (1956) 584-592.

[21] Z. Jiang, K. Takayama, An Investigation into the Validation of Numerical Solutions of Complex Flowfields, Journal of Computational Physics, 151 (1999) 479-497.

[22] Z.M. Hu, R.S. Myong, M.S. Kim, T.H. Cho, Downstream flow condition effects

on the RR → MR transition of asymmetric shock waves in steady flows, Journal of Fluid Mechanics, 620 (2009).